J Therm Anal Calorim (2012) 107:197–204
DOI 10.1007/s10973-011-1869-y

Thermal, structural and magnetic studies on chromite spinel synthesized using citrate precursor method and annealed at 450 and 650 °C

Rakesh K. Singh · A. Yadav · A. Narayan · Amrendra K. Singh · L. Verma · R. K. Verma

29th STAC-ICC Conference Special Chapter

Abstract Chromite Spinel materials were synthesized in this study by the citrate precursor method using four divalent cations (Ni^{2+}, Co^{2+}, Zn^{2+}, and Cu^{2+}). Citrate precursors consisting of mixed chromium citrates were first subjected to a thermogravimetric (TG) analysis for determining optimum temperatures for annealing. TG of co-precipitated chromium(III) citrate–zinc citrate gel has been carried out separately in N_2 and O_2 atmospheres. In both the cases, dehydration is followed by a four-step decomposition. The TG data were subjected to kinetic/mechanistic analysis, and the values of activation energy and Arrhenius factor were approximated. TG curves of various powders which were obtained on annealing at the two temperatures did exhibit thermal instability when carried out in N_2 atmosphere. A large coercivity of 2701.01 Oe was observed for $NiCr_2O_4$ at 650 °C. On the basis of the results, 450 °C has been chosen for annealing treatment of the four gels. The samples were accordingly annealed at two different temperatures (450 and 650 °C) in a muffle furnace for 1 h in each case. The annealed powders were characterized using X-ray diffraction (XRD), SEM, and vibrating sample magnetometer (VSM). The XRD patterns show that annealing of $CuCr_2O_4$, $NiCr_2O_4$, and $CoCr_2O_4$ at 450 °C yields very small crystallites with poor Bragg reflections, although $ZnCr_2O_4$ samples show better peaks in XRD data. Annealing at 650 °C resulted in particle size range of 8–89 nm in the four cases. In the case of $ZnCr_2O_4$, the particle size was 8 nm.

Keywords Chromites · Annealing · TG-DSC · XRD · SEM · Coercivity · Thermal stability · Kinetic parameters

R. K. Singh
Department of Physics, Patna Women's College, Patna University, Patna 800 001, India

A. Yadav
Vidya Vihar Institute of Technology, Purnea 854 301, India

A. Narayan
Department of Physics, Patna University, Patna, Bihar 800 005, India

A. K. Singh · L. Verma · R. K. Verma (✉)
University Department of Chemistry, Magadh University, Bodh Gaya 824 234, India
e-mail: profrkverma@gmail.com

Introduction

Transition metal and rare earth oxides have been known to exhibit interesting magnetic, electrical, and catalytic properties bringing tremendous potentialities to these materials. Lanthanum chromites [1], for example, have been used as interconnect material in solid oxide fuel cells. Copper chromite can be cited as another example which has emerged as an effective catalyst for use with composite solid propellants used for propulsion of rockets [2] which imparts a pressure-independent catalytic effect on the burning rate of oxidizers such as ammonium perchlorate. Chromite in general (MCr_2O_4 where M is a divalent metal) is a common accessory mineral present in most meteorites and mantle rock. It crystallizes in cubic system, has a spinel structure, and has a low Curie temperature. The ternary metal oxide spinel has potential catalytic and chemical sensing applications [3–6]. Unlike ferrites, the chromite spinels have no B-site Fe^{3+}. Still, these are relevant in view of the principles involved as well as their technological applications. In addition, strong negative exchange interaction, J_{BB}(Cr–O–Cr) controls the magnetic behavior in the

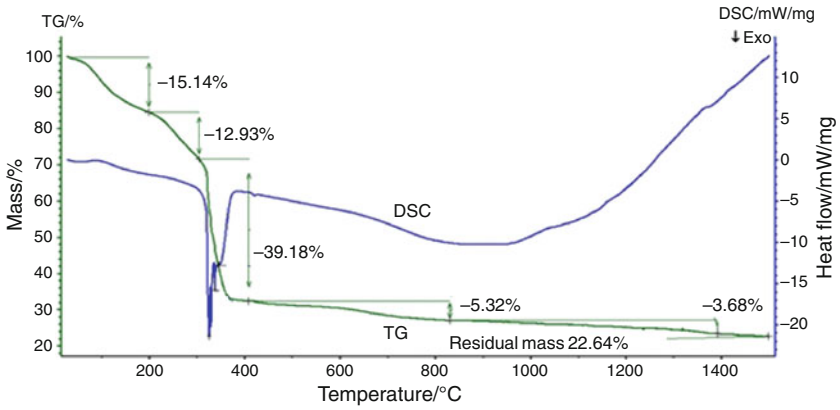

Fig. 1 TG-DSC curves of coprecipitated chromium(III) citrate–zinc citrate gel in O_2 atmosphere

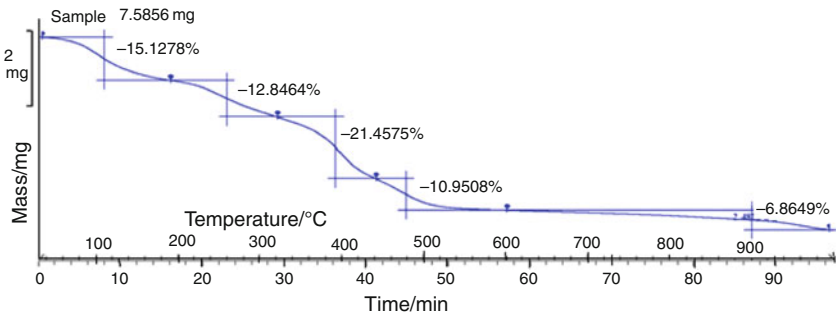

Fig. 2 TG curve of coprecipitated chromium(III) citrate–zinc citrate gel in N_2 atmosphere

Table 1 TG features shown by the chromium(III) citrate–zinc citrate gel

Steps	Temperature range/K	In N_2/% loss	In O_2/% loss	Best fitted mechanism	E_a/kJ mol^{-1}	ln A	$\Delta S^{\#}$/J K^{-1} mol^{-1}
I (dehydration)	333–463	15.13	15.14	2D diffusion	46.730	7.361	−186.12
II	473–593	12.85	12.93	3D diffusion	80.624	9.412	−171.49
III	603–713	21.46	39.18	2D diffusion	153.021	19.278	−91.21
IV	723–803	10.95	5.32	1st Order	49.456	26.407	−33.39
V	873–1170	6.86	3.68	–	–	–	–

chromite spinel [7, 8]. The magnetic and crystalline constant values for chromites have been presented earlier [9].

Several chromites have been synthesized in nanocrystal form so far. $ZnCr_2O_4$ crystallizes well when the sintering temperature is above 500 °C [3], and the product formed at 350 °C is in amorphous phase. The ceramic method has been used for this synthesis. Pure $MgCr_2O_4$ has been reported to have formed when appropriate mixture of pure oxides is pressed into bars and sintered for several hours in an electric furnace at 1,400 °C [10]. Some chromites, such as $MgCr_2O_4$, $CuCr_2O_4$, $NiCr_2O_4$, $ZnCr_2O_4$, and $CoCr_2O_4$, have been prepared using coprecipitation method, by the process of recrystallization from pyridine followed by ignition in the temperature range of 700–1,200 °C [7]. Nanometer size particles having perovskite structure were reported to be formed [1] when partial substitution by alkaline rare earth metals was carried out in lanthanum chromites by urea combustion method, and this was followed by calcination at 900 °C.

In the present study, thermal analysis of coprecipitated chromium(III) citrate–zinc citrate gel atmosphere has been carried out in N_2 and O_2 atmospheres and, on the basis of the results, 450 °C has been chosen for the annealing treatment of the four gels mentioned above. Annealing has also been done at 650 °C in an attempt to obtain nanometric particles of chromites (MCr_2O_4) {M = Cu, Ni, Zn, and Co} and to find out their magnetic properties which could render them useful for chemical sensing applications, etc. A comparison of the powders obtained at the two temperatures has also been made. Thermogravimetric (TG) data and their kinetic analysis provide clues to thermal stability, kinetics, and thermodynamics of the

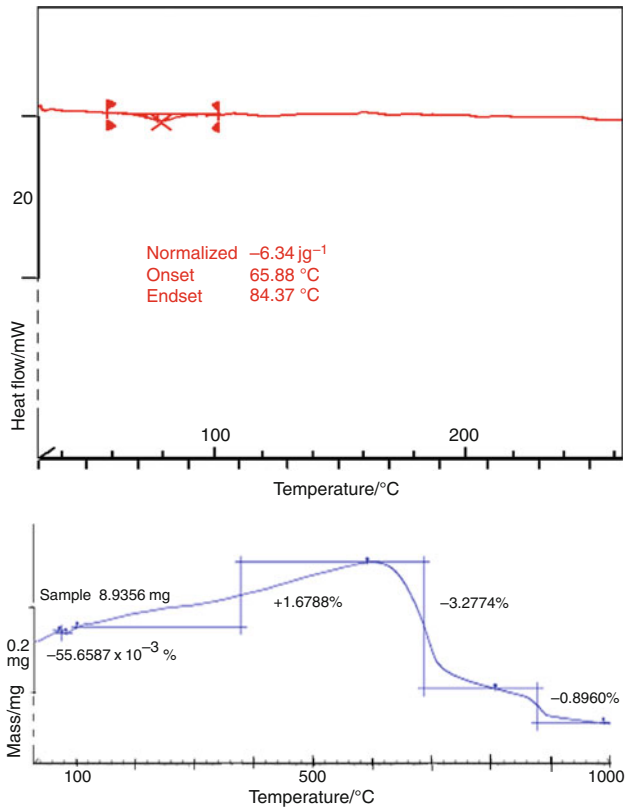

Fig. 3 TG-DSC curves (in N_2) of powder of copper chromite annealed at 650 °C

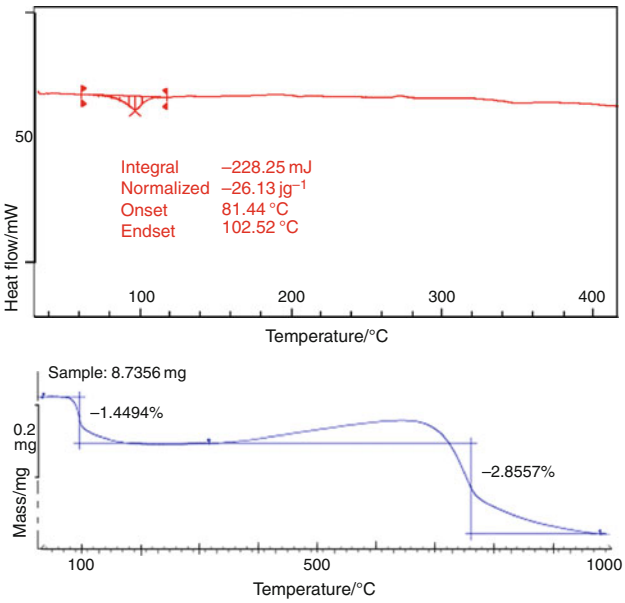

Fig. 4 TG-DSC curve (in N_2) of powder of nickel chromite annealed at 650 °C

decomposition of complexes and other compounds [11–22]. Phase changes caused by heating and influence of structure defects on reactivity can have significances [23, 24], and these may have implications on the applications of materials. In the present study, effort has been made to choose the annealing temperature on the basis of the TG data. On all the chromite samples the magnetization and retentivity are very small as expected. However, coercivity was found to change as the annealing temperature was increased.

Experimental

M $(NO_3)_n$ {M = Cu^{2+}, Ni^{2+}, Zn^{2+}, and Co^{2+}} and chromium(III) nitrate were taken as per stoichiometric requirements as the respective starting materials. Aqueous solution of the salt was prepared by dissolving it in minimal amount of deionized water while stirring constantly. The corresponding solutions were then mixed together. Aqueous solution of citric acid was prepared in adequate quantity by weight and was added to the prepared salt solutions. The mixture was heated at 60–80 °C for 2 h with continuous stirring. This solution was allowed to cool at room temperature and finally concentrated by heating at 60–65 °C in an oven until formation of a brown color fluffy mass. TG analysis of the precursor was

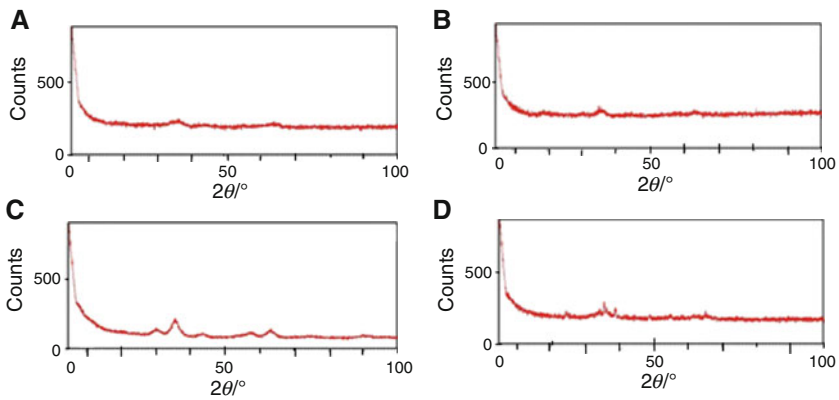

Fig. 5 XRD pattern of **a** $NiCr_2O_4$, **b** $CoCr_2O_4$, **c** $ZnCr_2O_4$, and **d** $CuCr_2O_4$ annealed at 450 °C for 1 h

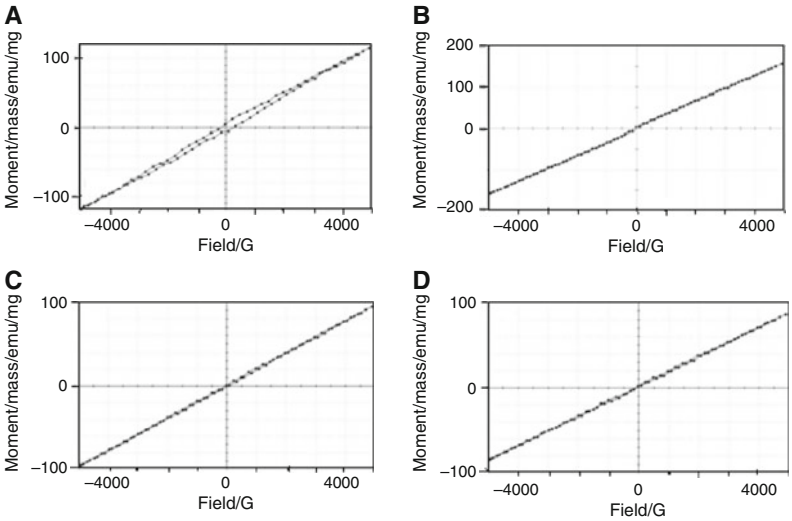

Fig. 6 Magnetization curves for **a** $NiCr_2O_4$, **b** $CoCr_2O_4$, **c** $ZnCr_2O_4$, and **d** $CuCr_2O_4$ annealed at 450 °C for 1 h

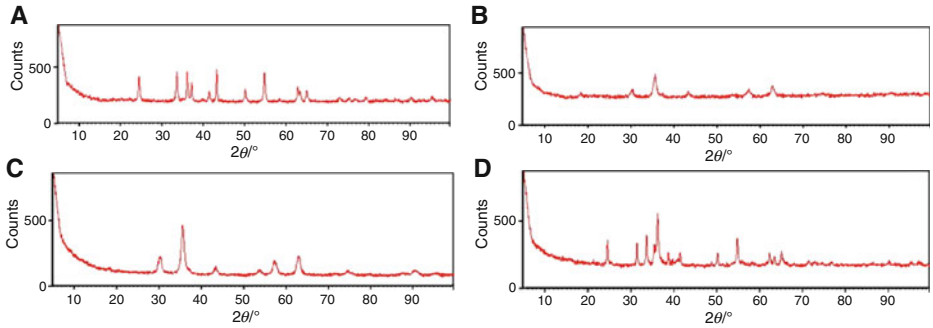

Fig. 7 XRD pattern of **a** $NiCr_2O_4$, **b** $CoCr_2O_4$, **c** $ZnCr_2O_4$, and **d** $CuCr_2O_4$ annealed at 650 °C for 1 h

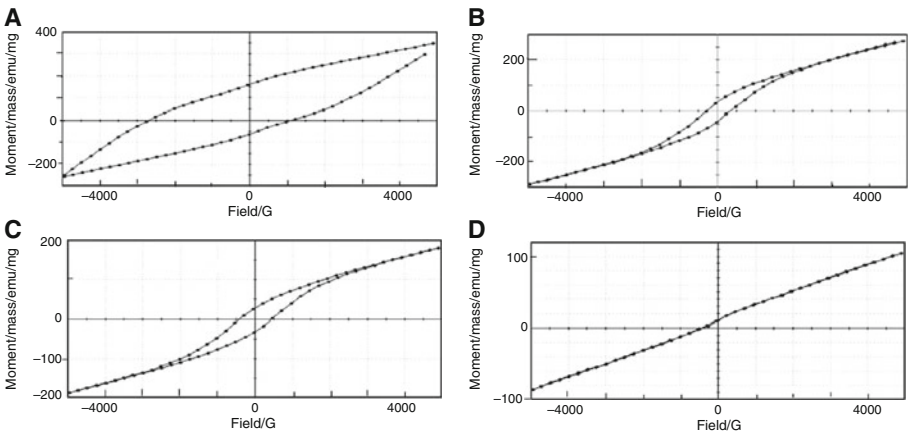

Fig. 8 Magnetization curves for **a** $NiCr_2O_4$, **b** $CoCr_2O_4$, **c** $ZnCr_2O_4$, and **d** $CuCr_2O_4$ annealed at 650 °C for 1 h

Table 2 Observed XRD and magnetic data of the four chromites annealed at 450 and 650 °C

Observed parameters	$ZnCr_2O_4$		$NiCr_2O_4$		$CuCr_2O_4$		$CoCr_2O_4$	
	450 °C	650 °C	450 °C	650 °C	450 °C	650 °C	450 °C	650 °C
Phase (A = amorphous, N = nanocrystalline)	A	N	A	N	N	N	A	N
Crystalline size/nm	–	8	–	89	29	24	–	12
Coercivity/G	37.12	408.32	154.30	2701	109.69	451.69	59.620	268.98
Retentivity/emu/g	1.045E−3	29.075E−3	5.275E−3	0.112	2.300E−3	10.065E−3	2.346E−3	33.462E−3
Magnetization/emu/g	840.14E−6	0.1837	0.11232	0.381	84.899E−3	95.315E−3	0.15624	0.28045

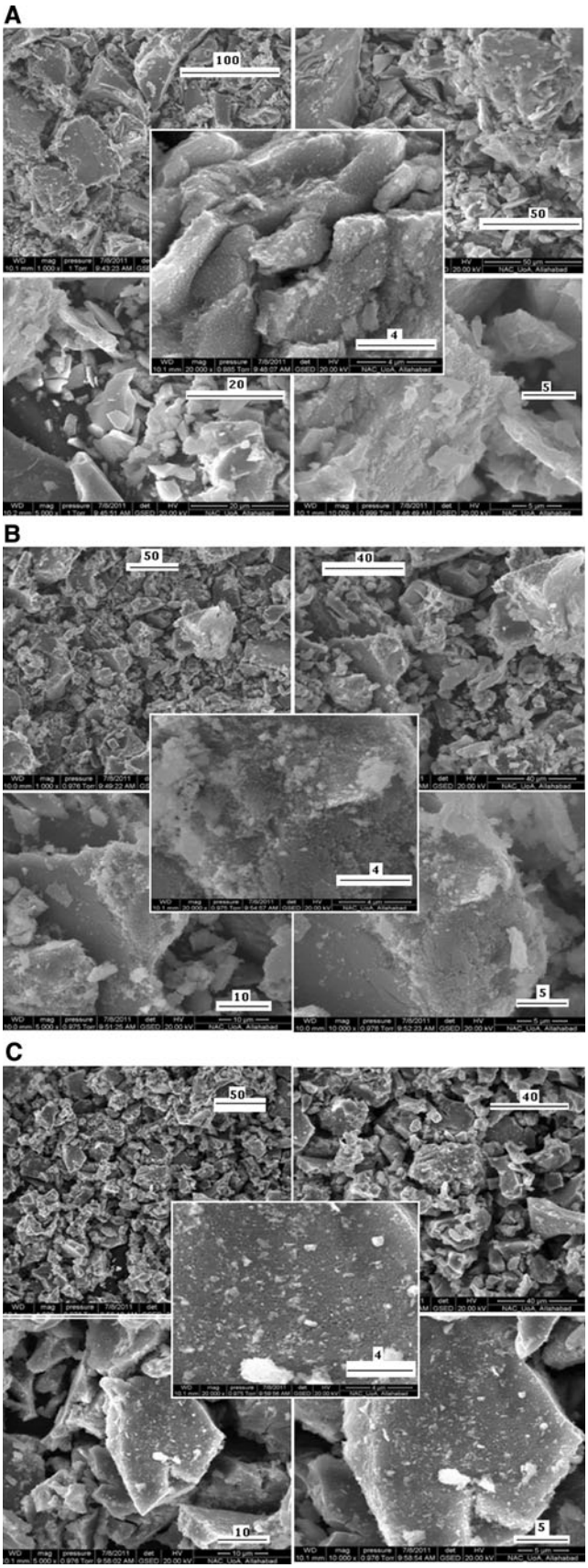

Fig. 9 **a** SEM of $CoCr_20_4$ obtained upon annealing at 650 °C (the scale depiction is in μm in the picture). **b** SEM of $NiCr_20_4$ obtained upon annealing at 650 °C (the scale depiction is in μm in the picture). **c** SEM of $CuCr_20_4$ obtained upon annealing at 650 °C (the scale depiction is in μm in the picture). **d** SEM of $ZnCr_20_4$ obtained upon annealing at 650 °C (the scale depiction is in μm in the picture). **e** SEM of $CuCr_20_4$ obtained upon annealing at 450 °C (the scale depiction is in μm in the picture)

carried out in oxygen at heating rate of 10 °C/min. The sample of zinc citrate gel was dehydrated by heating up to 200 °C, and the measurement was carried out without removing the sample from the instrument up to the desired temperature range using O_2 gas (Fig. 1). The process was repeated at 10 °C/min in alumina crucible using N_2 as the purge gas (Fig. 2). The initial two steps were common indicating no oxidation up to 330 °C. The third step ends around 450 °C. In total, the thermal decomposition has been found to be taking place in five steps. All the gels were annealed separately at two different temperatures (450 and 650 °C) for 1 h in a muffle furnace. By this process, the precursor was thermally decomposed to give a powder that was later characterized using X-ray diffractometer (XRD), SEM, and vibrating sample magnetometer (VSM). TG curves were also obtained for the annealed powders. Stoichiometry of all the annealed powders was confirmed to be MCr_2O_4 on the basis of percentage of metals. Kinetic studies have been undertaken on the precursor using TG data. The thermal analyses were carried out on Mettler TGA and NETZSCH STA 449F3 instruments. Scherrer Formula ($D = 0.9\ \lambda/\beta\ \cos\theta$) was used to calculate the particle size [25]. SEM (Model: Quanta 200 MK 2 Series FEI) was used for confirming the crystallite sizes (1000, 2000, 5000, 10,000, and 20,000 magnifications).

Results and discussion

Thermal analysis

The TG curves (Figs. 1, 2) of coprecipitated chromium(III) citrate–zinc citrate gel show five-step decomposition including dehydration in both the gaseous atmospheres (N_2 and O_2). The first two steps (ending at 330 °C) are identical. The third step involves oxidation when the purge gas is O_2. This step shows three peak temperatures (325.1, 337.1, and 346 °C) in the DSC curve. A clear horizontal appears around 450 °C, and hence this temperature was chosen for annealing of the four gels. Annealing has also been done at 650 °C. The activation energy is quite high in the steps following dehydration (Table 1). The kinetic trio

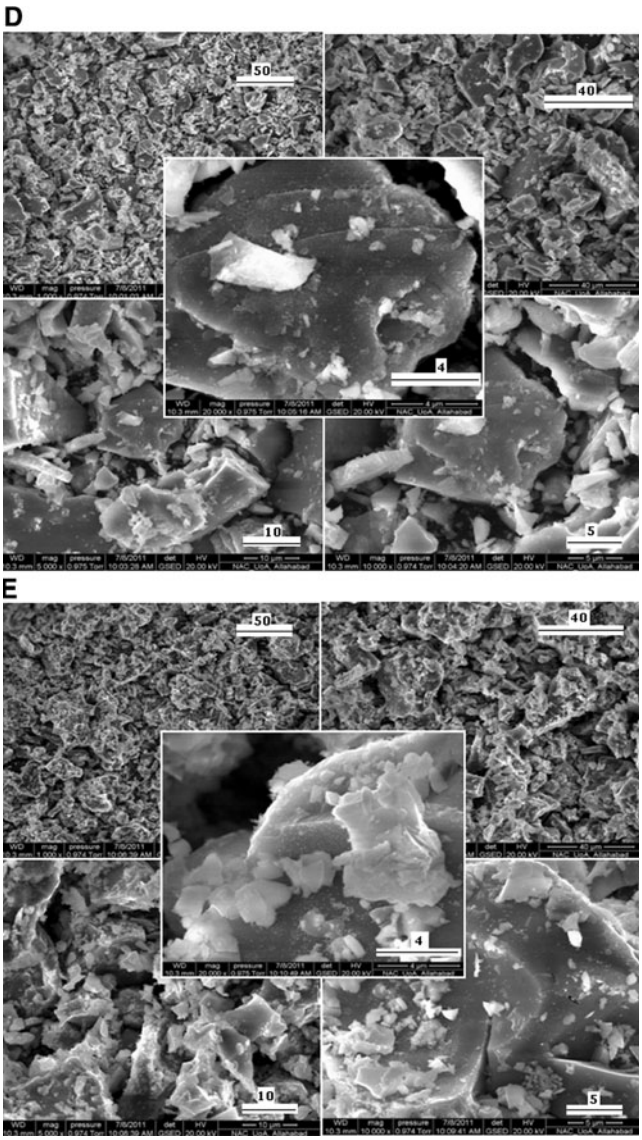

Fig. 9 continued

has been approximated from the most linear plot [19, 26] of ln k vs. $1/T$ using the following relation:

$$\ln k = \ln A - E/RT$$

where, ln k = ln $\{(d\alpha/dt)/f(\alpha)\}$. The values of $\Delta S^{\#}$ were approximated using the thermodynamic equation:

$$\Delta S^{\#} = R \ln Ah/kT$$

where $\Delta S^{\#}$ is the entropy of activation, A the frequency factor, R is the gas constant, k the Boltzmann constant, and T is the temperature at which $\alpha = 0.5$.

Gaseous adsorption, dissociation, and other catalytic properties of the copper chromite spinel surfaces have been reported [27]. N_2-adsorption is used to help us understand surface morphology, and this has been done for copper chromites and similar materials obtained by other methods [28–30]. Reductive deoxygenation in N_2 atmosphere of chromites has also been reported [31]. In the case of the powder of copper chromite annealed at 650 °C, N_2-adsorption is evident up to 600 °C after which dissociation is taking place (Fig. 3). Similarly, annealing at 650 °C makes the nickel chromite adsorb N_2 up to 640 °C and further heating causes dissociation (Fig. 4). No O_2-adsorption is taking place in any of the eight samples.

XRD, SEM, and magnetic studies

The XRD patterns and the magnetization curves of the samples annealed at temperature 450 °C are shown in Figs. 5 and 6, respectively. Amorphous chromites (except copper chromite which is in poor crystalline state) are formed when the annealing is done at 450 °C. An annealing temperature of 500 °C has been found to be necessary for fully incorporating the divalent metal into spinel phase while preparing ferrites [8]. The XRD patterns and room temperature magnetization curves for the samples annealed at temperature 650 °C are shown in Figs. 7 and 8, respectively. The observed data have been incorporated in Table 2. The coercivity, retentivity, magnetization, and hysteresis loop area have been observed to be increasing in nickel, zinc, and cobalt chromites, with the annealing temperature increasing from 450 to 650 °C. Copper compounds sometimes exhibit interesting magnetic properties which are accounted for on the basis of their structure [32].Here also; the copper chromite shows small magnetization (0.28045 emu/g) and appears in particle size of 24 nm (Table 2). The remaining chromites have small magnetization at 650 °C, but no crystals are formed at 450 °C. Four hours of annealing has been reported to be yielding stoichiometrically pure powder of $NiCr_2O_4$ [33]. XRD studies have earlier confirmed the absence of reactant oxides of NiO, Fe_2O_3, and Cr_2O_3. Tetragonal structure below 47 °C is believed to be because of Jahn–Teller effect. In the present study, $NiCr_2O_4$ has shown the highest coercivity of 2,701 G, while magnetization and retentivity values are at 0.381 emu/g and 0.1123 emu/g, respectively. $ZnCr_2O_4$ had minor amounts of ZnO when slurried mixture was dried at 120 °C followed by calcination at 650 °C. A mixed oxide of iron and chromium was also present [34]. The $ZnCr_2O_4$ particles furnished in the present study have small crystallite size of 8 nm and have maximum coercivity and magnetization values (408 G and 0.1837 emu/g, respectively). These results for the sizes have been supported by SEM studies (Fig. 9) on the four samples annealed at 650 °C, and the $CuCr_2O_4$ sample obtained upon annealing at 450 °C.

Conclusions

- TG curves of coprecipitated chromium(III) citrate–zinc citrate gel show five-step decomposition including dehydration in both the gaseous atmospheres (N_2 and O_2). The first two steps (ending at 330 °C) are identical. The third step involves oxidation when the purge gas is O_2. The activation energy is quite high in the steps after dehydration.
- In the case of copper chromite powder annealed at 650 °C, N_2-adsorption is evident up to 600 °C, after which dissociation takes place. Similarly, annealing at 650 °C makes the nickel chromite adsorb N_2 up to 640 °C, and further heating causes dissociation (Fig. 4). No O_2-adsorption takes place in any of the eight samples.
- Using the citrate precursor method, $CuCr_2O_4$ has been obtained in nanocrystalline phase of particle size 29 nm when the annealing temperature is 450 °C. $ZnCr_2O_4$ is furnished in particle size of 8 nm when the annealing temperature is 650 °C. The SEM studies support the findings though particle size is not uniform.
- Largest coercivity 2,701 G was observed for $NiCr_2O_4$ which did show retentivity and magnetization of 0.112 emu/g and 0.381 emu/g, respectively.

Acknowledgements The authors are thankful to Dr. R. K. Kotnala, Head, Magnetic Lab, the National Physical Laboratory (NPL), New Delhi for magnetization measurements, Prof Avinash Chandra Pandey of University of Allahabad (India) for providing SEM facilities, and Mr Mahesh (Mettler) and Ms Priya (Netzsch) for the recording of TG curves. The first and the second authors are also thankful to the Nalanda Open University, Patna for extending a partial financial support for this study.

References

1. Marinho EP, Souza AG, de Melo DS, Santos IMG, Melo DMA, da Silva WJ. Lanthanum chromites partially substituted by calcium, strontium and barium synthesized by urea combustion. J Therm Anal Calorim. 2007;87:801–4.
2. Tagliaferro FS, Fernandes EAN, Bacchi MA, Campos EA, Dutra RCL, Diniz MF. INAA for validation of chromium and copper determination in copper chromite by infrared spectrometry. J Radioanal Nucl Chem. 2006;269:403–6.
3. Chen XH, Zhang HT, Wang CH, Luo XG, Li PH. Effect of particle size on magnetic properties of zinc chromite synthesized by sol-gel method. Appl Phys Lett. 2002;81:4419–21.
4. Hagemann IS, Huang Q, Gao XPA, Ramirez AP, Cava RJ. Geometric magnetic frustration in $Ba_2Sn_2Ga_3ZnCr_7O_{22}$: a two dimensional spinel based Kagome lattice. Phys Rev Lett. 2001; 86:894–7.
5. Schwickardi M, Johann T, Schmidt W, Schuth F. High surface area oxides obtained by an activated carbon route. Chem Mater. 2002;14:3913–9.
6. Barreca D, Comini E, Ferrucci AP, Gasparroto A, Maccato C, Maragno C, Sberveglieri G, Tondello E. First example of ZnO–TiO_2 nanocomposites by vapor deposition: structure, morphology, composition and gas sensing performances. Chem Mater. 2007;19:5642–9.
7. West AR. Solid state chemistry and its applications. New Delhi: Wiley India; 2007. pp 6–17.
8. Bandopadhay AK. Nanomaterials. Delhi: New Age International Publishers; 2009. p 172.
9. Chikazimi S. Physics of ferromagnetism. 2nd ed. New York: Oxford University Press; 1997. pp 206–7.
10. Verway EJW, Heilmann EL. Cation arrangement in spinels. J Chem Phys. 1947;15(4):174–80.
11. Verma RK, Verma L, Chandra M. Thermoanalytical studies on the non-isothermal dehydration and decomposition of dl-lactates of a series of transition metals. Indian J Chem. 2003;42A:2982–7.
12. Bhattacharjee NC, Kumar M, Kumar S, Verma RK. Kinetic and mechanistic studies on non-isothermal decomposition of potassium dioxalatocuprate(II) dihydrate. J Indian Chem Soc. 1998;75(5):317–8.
13. Verma RK, Verma L, Chandra M, Bhushan A. Non-isothermal dehydration and decomposition of dl-lactates of transition metals and alkaline earth metals: a comparative study. J Therm Anal Calorim. 2005;80:351–4.
14. Tanaka H, Brown ME. The theory and practice of thermoanalytical kinetics of solid state reactions. J Therm Anal Calorim. 2005;80:795–7.
15. Brown ME, Gallagher PK. Introduction to recent advances, techniques and applications of thermal analysis and calorimetry. In: Brown ME, Gallagher PK, editors. Hand book of thermal analysis and calorimetry. Amsterdam: Elsevier; 2008. p. 1–12.
16. Verma RK, Verma L, Chandra M, Verma BP. Kinetic parameters of thermal dehydration and decomposition from thermoanalytical curves of zinc dl-lactate. J Indian Chem Soc. 1998; 75:162–4.
17. Verma BP, Verma RK, Chandra M, Pandey S, Mallick AK, Verma L. A study of non-isothermal decomposition of calcium dl-lactate pentahydrate. Asian J Chem. 1994;6:606–12.
18. Verma RK, Verma L, Ranjan M, Verma BP, Mojumdar SC. Thermal analysis of 2-oxocyclopentanedithiocarboxylato complexes of iron(III), copper(II) and zinc(II) containing pyridine or morpholine as the second ligand. J Therm Anal Calorim. 2008; 94:27–31.
19. Verma RK, Verma L, Bhushan A, Verma BP. Thermal decomposition of complexes of cadmium(II) and mercury(II) with triphenylphosphanes. J Therm Anal Calorim. 2007;90:725–9.
20. Verma RK, Mishra BK, Satpathy KC, Mahapatra A. Synthesis and characterization of mono and homo-dinuclear, cobalt(II), nickel(II) and copper(II) complexes of the schiff base derived from 3-formylsalicyclic acid and hydroxylamine hydrochloride. Asian J Chem. 1997;9(3):365–71.
21. Kumar M, Verma RK, Verma L, Bhattacharjee NC, Kumar S, Verma BP. Thermal decomposition of potassium trioxalato chromate(III) trihydrate: a kinetic and mechanistic study. Asian J Chem. 1996;8(3):543–6.
22. Agrawal HL, Mishra A, Ambasta RK, Verma L, Verma RK, Verma BP. Kinetic parameters of thermolysis of complexes of rhodium(III), palladium(II) and platinum(II) with substituted morpholines from their non-isothermal thermogravimetric data. Asian J Chem. 1994;6:130–4.
23. Marinescu C, Sofronia A, Rusti C, Piticescu R, Badilita V, Vasile E, Baies R, Tanasescu S. DSC investigation of nanocrystalline TiO_2 powder. J Therm Anal Calorim. 2011;103:49–57.
24. Jesenac V, Turcaniova L, Tkacova K. Kinetic analysis of thermal decomposition of magnesite: influence of generated defects and their annealing. J Therm Anal Calorim. 1997;48:93–106.
25. Cullity BD. Elements of X-ray diffraction. New York: Wiley; 1978. p. 101.

26. Samtani M, Dollimore D, Alexander KS. Comparison of dolomite decomposition kinetics with related carbonates and the effect of procedural variables on its kinetic parameters. Thermochim Acta. 2002;392–393:135–45.
27. Jalowiecki L, Wrobel G, Daage M, Bonnelle JP. Structure of catalytic sites of hydrogen treated copper containing spinel catalysts. J Catal. 1987;107:375–92.
28. Liang C, Ma Z, Ding L, Qiu J. Template preparation of highly active and selective Cu–Cr catalysts with high surface area for glycerol hydrogenolysis. Catal Lett. 2009;130:169–76.
29. Nakoumbou C, Villieras F, Barres O, Bihannic J, Pelletier M, Razafitianamaharavo A, Metang V, Yonta NC, Njopwouo D, Yvon J. Physicochemical properties of talc ores from Pout-Kelle and Memel deposits. Clay Miner. 2008;43:317–37.
30. Comino G, Gervasini A, Ragaini V, Ismagilov ZR. Methane combustion over copper chromite catalysts. Catal Lett. 1997;48: 39–46.
31. Fouad NE. Formation of Cr(II) species in the H_2/CrO_3 system parameter control. J Therm Anal Calorim. 2000;60:541–7.
32. Varma RC, Varma K, Verma RK, Bhattacharjee NC. Synthesis and characterization of copper(II) complexes of 4-amino-3-hydrazino-5-mercapto-1,2,4-triazole. J Indian Chem Soc. 1992; 69:577–8.
33. Ziemniak SE, Gaddipati AR, Sander PC. Immiscibility in the $NiFe_2O_4$–$NiCr_2O_4$ spinel binary. J Phys Chem Solids. 2005;66: 1112–21.
34. Kehl WL. US Patent # 3595810. 1971 (July 27).